**ISSN** 1672-9145 **Acta Biochimica et Biophysica Sinica** 2007, **39**(9): 657–667 **CN** 31-1940/Q

# Hyperhomocysteinemia-mediated DNA Hypomethylation and its Potential Epigenetic Role in Rats

Yideng JIANG[1]*, Tao SUN[1], Jiantuan XIONG[1], Jun CAO[1], Guizhong LI[1], and Shuren WANG[2]

[1] *Department of Pathophysiology, Ningxia Medical College, Yinchuan 750004, China;*
[2] *Department of Pathophysiology, West China College of Preclinical and Forensic Medical Sciences, Sichuan University, Chengdu 610041, China*

**Abstract** Hyperhomocysteinemia (HHcy), which is an independent risk factor for atherosclerosis, might cause dysregulation of gene expression, but the characteristics and key links involved in its pathogenic mechanisms are still poorly understood. The objective of the present study was to investigate the effect of HHcy on DNA methylation and the underlying mechanism of homocysteine (Hcy)-induced DNA methylation. HHcy was induced in Sprague-Dawley rats after 4 weeks of a low, medium or high methionine diet. The levels of total homocysteine, S-adenosylmethionine (AdoMet) and S-adenosylhomocysteine (AdoHcy) were detected by high-performance liquid chromatography. The expression levels of genes and proteins of S-adenosylhomocysteine hydrolase, DNA methyltransferase and methyl-CpG-binding domain 2 were detected by real-time reverse transcription-polymerase chain reaction and Western blot analysis. A high-throughput quantitative methylation assay using fluorescence-based real-time polymerase chain reaction was employed to determine the levels of DNA methylation. The results indicated that HHcy induced the elevation of AdoHcy concentration, the decline of AdoMet concentration, the ratios of AdoMet/AdoHcy and the RNA and protein expression of S-adenosylhomocysteine hydrolase and methyl-CpG-binding domain 2, as well as an increase of DNA methyltransferase activity. With different methylation-dependent restriction endonucleases, the aberrant demethylation was found to prefer CCGG sequences to CpG islands. Increasing levels of HHcy significantly increased genome hypomethylation in B1 repetitive elements. The impacts of different levels of HHcy showed that the varied detrimental effects of HHcy could be attributed to different concentrations through different mechanisms. In mild and moderate HHcy, the Hcy might primarily influence the epigenetic regulation of gene expression through the interference of transferring methyl-group metabolism. However, at high Hcy concentrations, the impacts might be more injurious through oxidative stress, apoptosis and inflammation.

**Keywords** hyperhomocysteinemia; DNA methyltransferase; DNA methylation; AdoMet; AdoHcy hydrolase

Homocysteine (Hcy) is a non-protein sulfur-containing amino acid that is formed exclusively upon demethylation of methionine, and it is a precursor of S-adenosylmethionine (AdoMet), the primary methyl group donor for most biological methylations, including DNA [1]. After transfer of the methyl group, AdoMet is converted to S-adenosylhomocysteine (AdoHcy), a potent inhibitor of many AdoMet-dependent methyltransferases [2]. Accumulating evidence over the past decade indicated that hyperhomocysteinemia (HHcy) is a common and independent risk factor for cardiovascular disorders [3,4] and strong association between HHcy and atherosclerosis has been observed in many retrospective and prospective studies [5]. The precise mechanisms of HHcy-inducing atherosclerosis, however, remain unknown. Much attention has been focused on characterizing the impacts

Received: March 20, 2007 Accepted: June 3, 2007
This work was supported by a grant from the Specialized Research Fund for the Doctoral Program of Higher Education of China (No. 20050610050)

Abbreviations: AdoHcy, S-adenosylhomocysteine; AdoMet, S-adenosylmethionine; C-5McTase, C-5 DNA methyltransferase; Hcy, homocysteine; AdoHcyH, S-adenosylhomocysteine hydrolase; HHcy, hyperhomocysteinemia; tHcy, total homocysteine

*Corresponding author: Tel, 86-0951-4083421; Fax, 86-0951-4081245 E-mail, jwcjyd@163.com

DOI: 10.1111/j.1745-7270.2007.00327.x

of HHcy on dysfunction and injury of vascular cells. Increasing evidence, however, indicated that HHcy might also be involved in regulating the expression of atherosclerosis-related genes through the interference of DNA epigenetic phenotype modification [6–11].

Hypomethylation is an early and consistent event in the development of several cancers [12,13], and is associated with advanced human atherosclerotic lesions. Some reports have shown recently that genomic hypomethylation is present in lesions of apolipoprotein E knockout mice and neointima of balloon-denuded New Zealand white rabbit aortas [14]. Hypomethylation occurs in some specific genes, such as the 15-lipoxygenase gene, estrogen receptor gene and extracellular superoxide dismutase gene in atherosclerosis [15,16]. Genomic DNA (gDNA) methylation involved in atherosclerosis has not been investigated. Clusters of unmethylated CpG dinucleotides occur in the 5′ regulatory region in more than 50% of human genes and they have been termed CpG islands [17]. They can serve as a surrogate marker for gDNA methylation [16]. The B1 repetitive elements comprise approximately 45% of the human genome [18,19]. They are interspersed throughout the genome and contain much of the CpG methylation that was found in normal human postnatal somatic tissues. Loss of DNA methylation in these sequences might account for most of the genomic hypomethylation [20–22].

To pinpoint the pathogenic mechanism of this disturbance caused by HHcy, in this study we assessed gDNA methylation changes by analyzing methylation of the B1 repetitive elements and estimating DNA methyl-accepting capacity by restriction analysis. We also examined the effects of HHcy on methionine cycle intermediates, the activity of S-adenosylhomocysteine hydrolase (AdoHcyH) that hydrolyzes the AdoHcy to Hcy, and the levels of DNA methyltransferase (DNMT) 3a, DNMT3b and methyl-CpG-binding domain (MBD) 2. These investigations show that the perturbation of DNA methylation is implicated in the molecular mechanisms of HHcy. The alteration of DNA methylation might be an important finding that could point to a mechanism against atherosclerosis. These data, for the first time, indicate the effect on DNA methylation of Hcy in the context of atherosclerosis.

## Materials and Methods

### Induction of HHcy in an animal model

Male Sprague-Dawley rats (Sichuan University Laboratories, Chengdu, China), aged 8 weeks, were divided into four groups ($n$=20 for each group) and maintained for 4 weeks on the following diets before experiments: (1) regular diet (control), regular rodent diet; (2) low methionine (Wuxi Benniu Biotechnology, Wuxi, China) diet, regular diet plus 1% methionine; (3) mid-methionine diet, regular diet plus 1.5% methionine; or (4) high methionine diet, regular diet plus 2% methionine. A previous study suggested that a high methionine diet for 4 weeks was sufficient to induce HHcy in rats [23]. All procedures were carried out in accordance with the Guidelines for the Care and Use of Laboratory Animals approved by the National Research Council (China).

### Determination of plasma total homocysteine (tHcy), AdoMet and AdoHcy concentrations

Plasma tHcy was measured by high-performance liquid chromatography and electrochemical detection as described previously [24]. Levels of AdoMet and AdoHcy in the aorta tissue were measured by high-performance liquid chromatography coupled to an ultraviolet detector as described previously [25]. Tissues were collected in ice-cold perchloric acid (0.4 M) immediately after the rats were euthanized, and samples were deproteinized by homogenization and centrifugation within 1 h. The clear supernatant fraction was stored at –80 ºC until analysis. AdoMet and AdoHcy standards were used to identify the elution peaks. AdoMet and AdoHcy values were normalized to cellular protein content that was determined using the Coomassie Brilliant Blue method [26].

### Real-time quantitative reverse transcription-polymerase chain reaction (RT-PCR) analysis of AdoHcyH, DNMTs, MBD2

The aorta tissue was pulverized in liquid nitrogen, and total RNA was isolated using Trizol reagent (Invitrogen, Grand Island, USA). Primers were designed with Primer Premier 5.0 software. The primer nucleotide sequences and probes are shown in **Table 1**. RNA was reverse transcribed by Revert aid first strand cDNA synthesis kit (MBI, Vilnius, Lithuania), and cDNA was used as the template for polymerase chain reaction (PCR). The real-time PCR was carried out using an FTC2000 real-time PCR detection system with the program as follows: 40 cycles at 95 ºC for 45 s, annealing temperatures (**Table 1**) for 45 s and 60 ºC for 60 s. The melting curve analysis was carried out over the range 55–95 ºC by monitoring 6-FAM fluorescence with increasing temperature (0.5 ºC increment changes at 10 s intervals). PCR-specific products were determined as a clear single peak at the

**Table 1 Primer sequences for reverse transcription–polymerase chain reaction analysis**

| Gene | Accession No. | Primer and probe sequence | Length (bp) | Temperature (ºC) * |
|---|---|---|---|---|
| *AdoHcyH* | BC015304 | Forward primer: ACTGCCCTACAAAGTCGC | 393 | 54.8 |
| | | Reverse primer: CCTACTACCACCACTGGA | | |
| | | Probe sequence: TCCCACGAGCGTAACGACCG | | |
| *DNMT3b* | NM010068 | Forward primer: ACCCAACAAGAAGCAACC | 408 | 55.8 |
| | | Reverse primer: CCTCACAGACCTCCACGA | | |
| | | Probe sequence: GTGGTTGTTGTTCCCGTTAGAC | | |
| *DNMT3a* | NM007872 | Forward primer: ACCGCAAAGCCATCTACGA | 350 | 55.8 |
| | | Reverse primer: TCCCTCGCCGACCACATA | | |
| | | Probe sequence: GGCGTTTCGGTAGATGCTTCAG | | |
| *MBD2* | NM010773 | Forward primer: CAGCGGATGAATGAACAAC | 244 | 52.2 |
| | | Reverse primer: TGGGACGACAAACCGAAT | | |
| | | Probe sequence: TGCTTGGTGGGCTCGTTATT | | |

* annealing temperature. AdoHcyH, S-adenosylhomocysteine hydrolase; DNMT, DNA methyltransferase; MBD, methyl-CpG-binding domain.

melting curves above 80 ºC. The RNA level of each gene was acquired from the value of the threshold cycle (*Ct*) of the real-time PCR as related to that of *GAPDH* through **Equation 1**:

$$\Delta Ct = Ct(\text{GAPDH}) - Ct(\text{sample}) \quad (1)$$

Final results, expressed as N-fold differences in target gene expression relative to the calibrator, termed "$N_{\text{target}}$" were determined as **Equation 2**:

$$N_{\text{target}} = 2^{\Delta Ct(\text{sample}) - \Delta Ct\ (\text{calibrator})} \quad (2)$$

where $\Delta Ct$ values of the calibrator and sample were determined by subtracting the *Ct* value of the target gene from the *Ct* value.

### Western blot analysis of AdoHcy, DNMTs and MBD2

Electrophoresis (50 μg of protein from aorta tissue extracts) was carried out on sodium dodecyl sulfate-polyacrylamide gels. Proteins were transferred to nitrocellulose membranes at 67 V for 2 h at room temperature with gentle agitation on a platform shaker, and washed three times for 5 min/time in Tris-buffered saline plus Tween-20 (TBST). The membrane was then incubated with a monoclonal anti-AdoHcyH, DNMTs and MBD2 antibody (1:250 dilution) in 10 ml primary antibody dilution buffer with gentle agitation overnight at 4 ºC. It was then washed three times with TBST and incubated with a second antibody (goat anti-rabbit horseradish peroxidase-conjugated immunoglobulin G; Jackson ImmunoResearch, West Grove, USA) in phosphate-buffered saline at 1:2000 dilution containing 1% bovine serum albumin (New England Biolabs, Beverly, USA) for 1 h at room temperature. After being washed again three times with TBST, the membrane was incubated with 10 ml LumiGLO (New England Biolabs) with gentle agitation for 1 min at room temperature, then the excess developing solution was drained. The membrane was not allowed to dry out, but was wrapped in a plastic wrap and exposed to X-ray film.

### Estimating DNA methyl-accepting capacity by restriction analysis

The methyl-accepting capacity of gDNA was measured as the loss of unmethylated cytosine after gDNA was digested with methylation-sensitive endonucleases [17]. Two restriction endonucleases, which recognize unmethylated cytosine, were used: *Hpa*II, specific for CCGG sequences; and *Bss*HII for CpG rich islands (CGCGCG). Purified gDNA (5 μg) was digested overnight with 10-fold excess of *Hpa*II or *Bss*HII according to the manufacturer's protocols (New England Biolabs). Samples of undigested gDNA served as controls. The digested and undigested gDNA were treated with an EZNA Cycle-Pure kit (Omega, Guangzhou, China) and purified gDNA (0.5 μg) was used for DNA methyl-accepting capacity assay as follows: purified gDNA (0.5 μg), bacterial SssI methylase (2 U) and [methyl-$^3$H]AdoMet (3 μCi per sample) were incubated in buffer containing 50 mM NaCl, 10 mM Tris-HCl, pH 8.0, and 10 mM EDTA (final volume 25 μl) for 2 h at 37 ºC. The reaction was stopped by placing the tubes on ice. Then 25 μl aliquots from each reaction mixture were applied onto GF/C filter discs, and

counted by scintillation counting. The results are expressed as [methyl-$^3$H]incorporation/0.5 μg DNA.

### Sodium bisulfite-sequencing assay

The B1 element (V01561) primers were as follows: 5′-CCTCAAACTCAAAAATCCACC-3′ (forward), and 5′-GTTGGGTGTAGTGGTAATATATATTTTTAATTTTA-3′ (reverse). The PCR was carried out in a 25 μl reaction volume with 200 μM dNTPs, 0.5 μM of each forward and reverse PCR primer, 1×PCR buffer and 2.5 U *Taq* polymerase using the following PCR program: 95 ºC for 5 min, then 35 cycles of 95 ºC for 15 s, 55 ºC for 30 s and 72 ºC for 2 min. PCR products were cloned using the TOPO-TA cloning kit (Stratagene, La Jolla, USA). The plasmid that had been fully methylated and unmethylated acted as the standard sample product. To generate a standard curve, we prepared different ratios of methylated versus unmethylated target sequences. The following ratios were prepared (methylated/unmethylated): 0/100, 10/90, 25/75, 50/50, 75/25, 90/10 and 100/0, and each sample was examined by real-time PCR analysis in duplicate. We correlated the Δ*Ct* values with the predefined prevalence of methylated alleles. The curve had a sigmoid shape with a linear part in the range of 10%–90% of methylated DNA (**Fig. 1**). From this, we deduced an algorithm to calculate the methylation ratio of an unknown sample.

Bisulfite modification of gDNA has been described previously [22]. DNA (up to 2 μg) was diluted into 50 ml with distilled $H_2O$. After adding 5.5 ml of 3 M NaOH, the sample was incubated at 42 ºC for 20 min. Then 30 ml of 10 mM hydroquinone (Sigma, St. Louis, USA) and 520 ml freshly prepared 3 M sodium bisulfite, pH 5.0 (Sigma) was added to each tube. After mixing together with the DNA, mineral oil was laid over the top the mixture was incubated at 50 ºC for 16 h. Following bisulfite conversions, the DNA was recovered using the Wizard DNA Clean-up system (Omega) according to the manufacturer's instructions with the following changes. After washing with 2 ml of 80% (*V*/*V*) isopropanol, the column was placed into a clean, labeled 1.5 ml tube and 50 ml of heated water (60–70 ºC) was added. The tube/column was spun in a Microfuge for 1 min, then 5.5 ml of 3 M NaOH was added to each tube, and the mixture was incubated at room temperature for 5 min. One milliliter of glycogen as carrier, 33 ml of 10 M $NH_4Ac$, and 3-fold volumes of ethanol were added into the mixture. DNA was precipitated normally (incubated overnight at –20 ºC, spun for 30 min), washed with 70% ethanol, then the pellet was dried and resuspended in 20 ml water. The eluted DNA sample was stored at –20 ºC.

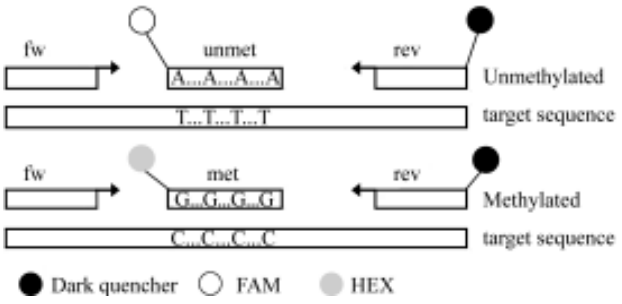


**Fig. 1 Schematic of the quantitative analysis of methylated alleles**

The bisulfite-treated target sequence is amplified with the same primer set irrespective of its methylation status. Two differently labeled internal MGB TaqMan1 probes bind to respective target and are cleaved by the 50 nuclease activity of *Taq* DNA polymerase. The amount of fluorescence dyes VIC and FAM released during polymerase chain reaction (PCR) is directly proportional to the amount of PCR product generated from the methylated or unmethylated allele, respectively. fw, forward primer; met, methylated probe; rev, reverse primer; unmet, unmethylated probe

A novel quantitative analysis of methylated alleles was used that is essentially a major improvement over a previous method based on real-time PCR (MethyLight) [23]. We used a VIC-labeled probe that specifically hybridizes to the sequence derived from the methylated allele, and a FAM-labeled probe that binds to the sequence generated from the unmethylated allele. The amount of fluorescent dye released during PCR is measured by a real-time PCR system and is directly proportional to the amount of PCR product. Binding sites of the probes cover three differently methylated CpG dinucleotides. Their improved sequence specificity facilitates relative quantification of methylated and unmethylated alleles that are simultaneously amplified in a single tube.

PCR primers were designed to amplify the bisulfite-converted antisense strand of the B1 repetitive element. PCR primers, probes and the strategy for designing the MethyLight reaction are shown in **Figs. 1** and **2**. PCR was carried out using a 96-well optical tray with caps at a final reaction volume of 20 μl containing 10 μl TaqMan universal PCR master mix, 2 μl bisulfite-treated DNA, 2.5 μM of each primer of B1 element and 150 nM each of the fluorescently-labeled probes B1 element met and B1 element unmet. Initial denaturation at 95 ºC for 5 min to activate the AmpliTaq Gold DNA polymerase was followed by 40 cycles of denaturation at 95 ºC for 15 s and annealing and extension at 60 ºC for 1 min.

The MethyLight data specific for methylated repetitive elements were expressed as the percent of methylated reference values. The percent of unmethylated reference


**Fig. 2 Sequences of B1 element primers and probes**

The probes for modified B1 element are indicated by shaded boxes, and the polymerase chain reaction (PCR) primers for the B1 element sequence are indicated by arrows. The sequence of B1 element after sodium bisulfite modification is also shown. The solid line arrows indicate the extension direction. Methylated and unmethylated PCR have the same primers. Fluorescence detection was carried out by two passages. When PCR was carried out with methylation-modified gDNA, the fluorescence of the methylated probe was detected by the one passage the same as PCR with unmethylation-modified gDNA. The other kind of fluorescence of unmethylated probes was detected by the other passages. Upper row, original sequence; lower row, bisulfite modified sequence (for display, assume all CpG sites are methylated); +, CpG site; non-CpG "C" converted to "T"; >>>, left primer; <<<, right primer.

values were calculated similarly to a previous report [24], but with the following changes. If the percentage of methylated DNA molecules in a real-time PCR experiment is given by $c$, $\Delta Ct = Ct_{\text{FAM}} - Ct_{\text{HEX}} = \text{Log}_2[c/(1-c)]$. To account for the differential efficacy of the PCR (methylated/unmethylated) and probe activity, we restate the model as $\Delta Ct = a + b\text{Log}_2[c/(1-c)]$, where $a$ and $b$ represent the additional effects. The following equation was deduced from the results generated by the standard curve **(Fig. 3)**, $c = 100/[1+2[(2-\Delta\text{Ct})/0.68]$ ($a$=2, $b$=0.68). Each MethyLight reaction was carried out between three and six times, and the data are the mean percent of methylated or unmethylated reference values of the three measurements.

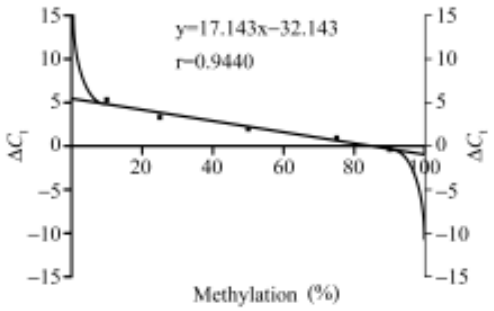


**Fig. 3 Standard curve as obtained by plotting the Δ*Ct* values against the predefined methylation ratio of each sample**

The standard deviation for each sample analyzed in duplicate is indicated. The *Ct* value was set to 40 in the case that the respective fluorescence signal did not cross the threshold. To set up the B1 element methylation assay, we mixed methylated DNA with unmethylated DNA prepared from T-A clone of the B1 element to generate DNA samples with defined ratios of unmethylated versus methylated B1 target sequences. We correlated the Δ*Ct* values with the predefined prevalence of methylated alleles. The curve has a sigmoid shape with a linear part in the range of 10%–90% of methylated DNA (**Fig. 1**); "y" and "r" represent the linear part. From this we deduced an algorithm to calculate the methylation ratio of an unknown sample from its Δ*Ct* value.

### Statistical analysis

Results are expressed as mean±SEM. The data were analyzed using one-way ANOVA and additional analysis was carried out using Student-Newman-Keuls's test for multiple comparisons within treatment groups, or Student's *t*-test between two groups. $P<0.05$ was considered significant.

## Results

### Concentrations of plasma tHcy, AdoMet and AdoHcy

After 4 weeks, plasma tHcy was mildly elevated in control mice ($P<0.05$) and markedly elevated in mice fed a high methionine diet ($P<0.001$) (**Fig. 4**). AdoMet and AdoHcy levels in aorta tissue are important impact factors in the transmethylation process. The levels of AdoHcy in low, mild or high methionine diet groups were significantly higher, up to 2- to 3-fold that of the control group. The concentrations of AdoMet were lower and the ratio

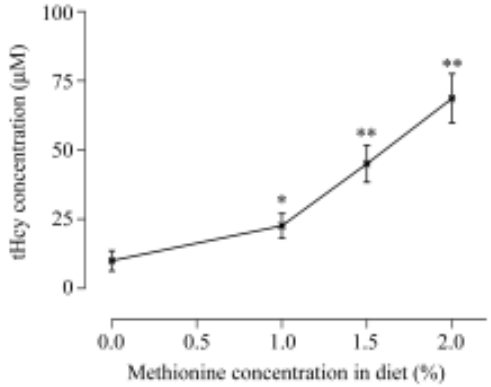


**Fig. 4 Levels of total plasma homocysteine (tHcy) in low, mild and high methionine diet groups**

0, Normal diet (regular diet plus 0% methionine); 1, low methionine diet (regular diet plus 1% methionine); 1.5, mid-methionine diet (regular diet plus 1.5% methionine); 2, high methionine diet (regular diet plus 2% methionine). **P*<0.05, ***P*<0.001 vs. normal group.

of AdoMet/AdoHcy in low, mild or high methionine diet groups was approximately 3- to 4-fold lower than the control group as the tHcy level increased (**Fig. 5**).

## RNA and protein expression analysis of AdoHcyH, DNMTs and MBD2

**Fig. 6** shows the relative RNA levels of AdoHcyH, DNMTs and MBD2 after normalization with GAPDH. These data show that the expression of AdoHcyH or MBD2 was down-regulated in all experimental groups, and was lower than the control group ($P<0.05$). AdoHcyH and MBD2 in the control group were 4.50- and 3.05-fold higher, respectively, than that in the low methionine diet group. DNMTs were up-regulated, and there was significant different between the control and experimental groups ($P<0.05$). Increasing concentrations of Hcy did not result in dose-dependent mRNA expression, and there was no significant difference of mRNA expression of AdoHcyH, DNMTs or MBD2 among low, mid or high methionine diet groups.

The effects of Hcy on protein level of AdoHcyH, DNMTs and MBD2 were measured by Western blot analysis (**Fig. 7**), which showed a result similar to the mRNA expression. The lowest protein expression of AdoHcyH was also in the low methionine diet group, and there was no significant difference of AdoHcyH, DNMTs or MBD2 protein levels among low, mid or high methionine diet groups.

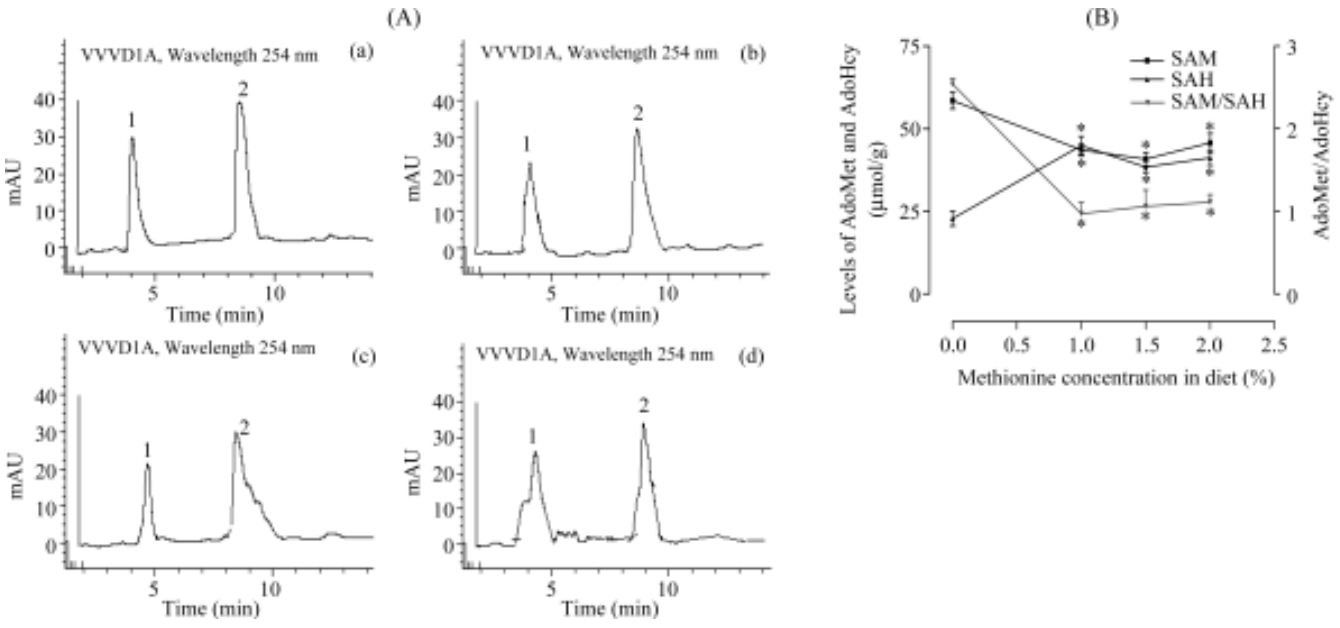


**Fig. 5 The contents of S-adenosylhomocysteine (AdoHcy) and S-adenosylmethionine (AdoMet) analysis**

(A) A chromatogram of S-adenosylhomocysteine (AdoHcy) and S-adenosylmethionine (AdoMet) of all groups. (a) Normal diet, control (0% methionine); (b) low methionine diet (1% methionine); (c) mid-methionine diet (1.5% methionine); (d) high methionine diet (2% methionine). Peak 1, AdoMet; peak 2, AdoHcy. The aorta tissue was homogenized in four volumes of 0.4 M $HClO_4$. The acid extract (200 μl) was applied directly onto the high-performance liquid chromatography. Chromatograms were recorded by integrators. (B) Effects of homocysteine on AdoHcy, AdoMet and AdoMet/AdoHcy. Quantification of AdoHcy and AdoMet were accomplished by automatic peak area integration. AdoMet and AdoHcy standards were used to identify the elution peaks. Results were mean±SE for three experiments. **P*<0.05 vs. control.

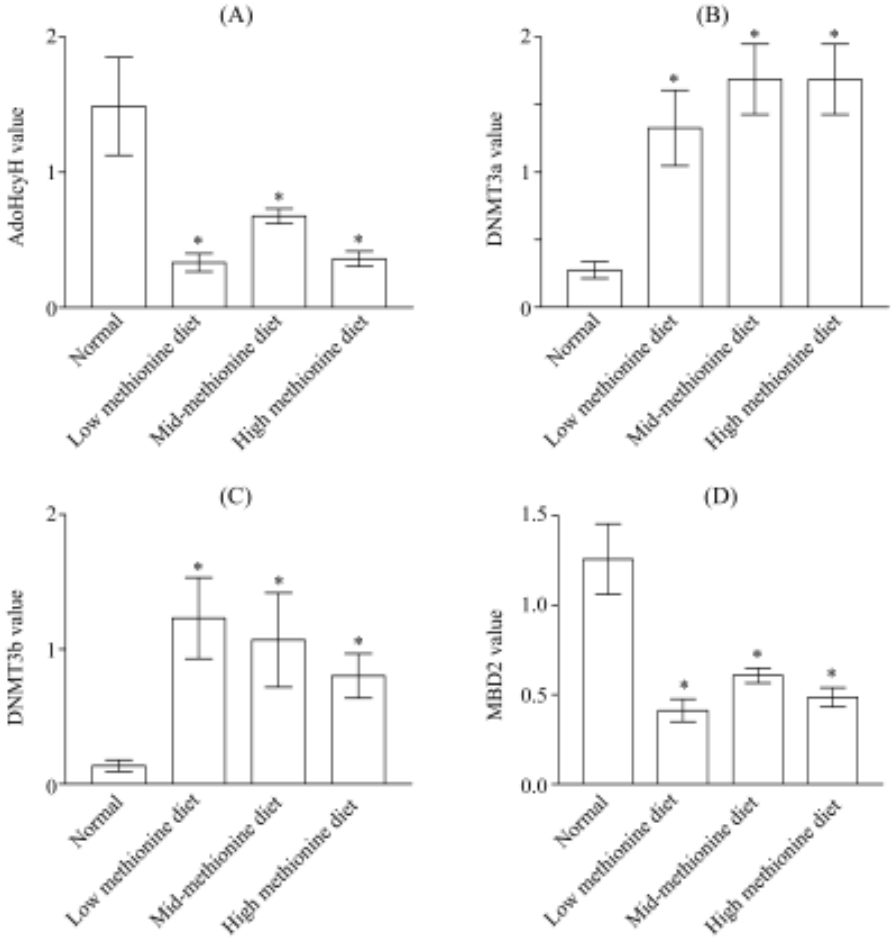


**Fig. 6 mRNA expression of S-adenosylhomocysteine hydrolase (AdoHcyH), DNA methyltransferase (DNMT)3a, DNMT3b, methyl-CpG-binding domain (MBD)2 and glyceraldehyde-3-phosphate dehydrogenase (GAPDH) by real-time polymerase chain reaction (PCR) analysis**

The relative mRNA levels of AdoHcyH (A), DNMT3a (B), DNMT3b (C) and MBD2 (D) after normalization. The fluorescence was plotted versus the PCR cycle number for both reactions and each sample dilution is indicated. Each gene RNA level was acquired from the value of the threshold cycle (*Ct*) of the real-time PCR as related to that of GAPDH through the formula $\Delta Ct$ [$\Delta Ct = Ct$(GAPDH) $- Ct$(sample)]. Final results, expressed as N-fold differences in target gene expression relative to the calibrator, termed "$N_{target}$" is determined as $N_{target} = 2^{-\Delta Ct}$(sample)$-2^{-\Delta Ct}$(calibrator), where $\Delta Ct$ values of the calibrator and sample were determined by subtracting the *Ct* value of the target gene from the *Ct* value. Data shown were representative of three separate experiments. $^*P<0.05$, compared with control group.

## DNA methylation-dependent restriction analysis

**Fig. 8** shows an increase of methyl-accepting capacity of gDNA without being digested by the restriction endonucleases in low, mid and high methionine diet groups. In the control group, the methyl-accepting capacity of gDNA showed a small, but not significant, decline, whereas in all experimental groups, the decrease in methyl-accepting capacity was significant. This decline indicated hypomethylation was induced by HHcy in gDNA. The greater decrease in methylation-accepting capacity was observed in groups with *Hpa*II digestion, and its reduction in methylation-accepting capacity was 70.1%, 41.7% and 46.1% for the low, mid and high methionine diet groups, respectively, compared with undigested DNA. The methylation-accepting capacity in *Bss*HII cutting groups declined approximately 45.5%, 8.1% and 7.4% for the low, mid and high methionine diet groups, respectively, compared with undigested DNA. The HHcy induced-demethylation also showed the highest effect in the low methionine diet group.

## Homocysteine-induced B1 repetitive elements methylation changes

MethyLight is a quantitative, TaqMan-based real-time PCR to measure DNA methylation profiles, using bisulfite-

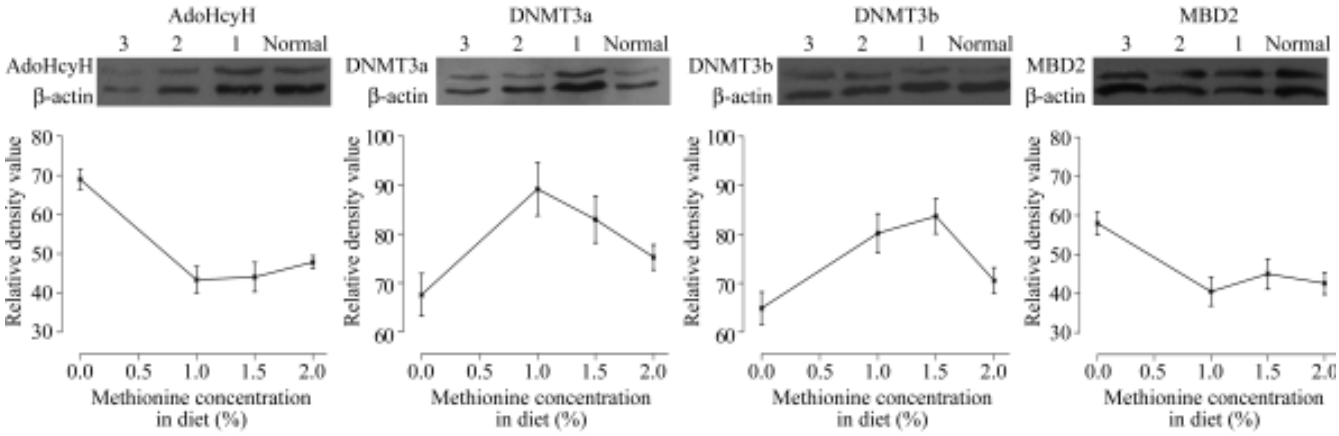


**Fig. 7 Effects of homocysteine on S-adenosylhomocysteine hydrolase (AdoHcyH), DNA methyltransferase (DNMT) and methyl-CpG-binding domain (MBD) 2 protein levels**

Western blots were analyzed by densitometry. Normal diet, control (0% methionine); 1, low methionine diet (1% methionine); 2, mid-methionine diet (1.5% methionine); 3, high methionine diet (2% methionine). The results were expressed as percentage of control±SEM (error bar). Each experiment was carried out in duplicate. The control value was expressed as 100%. Related value was related to that of β-actin through the formula (related value=experiment densitometry value×100/β-actin value). **P*<0.05 compared with control group.

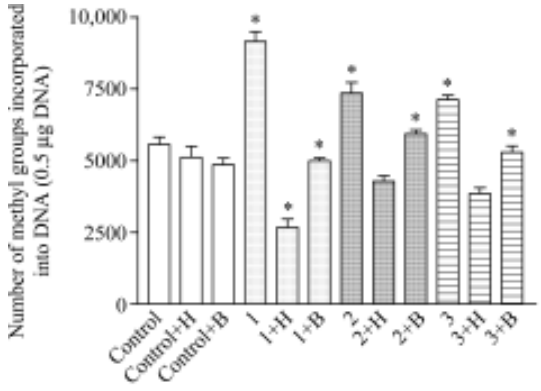


**Fig. 8 Capacity of genomic DNA undigested and digested with *Hpa*II (H) or *Bss*HII (B)**

Control, normal diet (0% methionine); 1, low methionine diet (1% methionine); 2, mid-methionine diet (1.5% methionine); 3, high methionine diet (2% methionine). Each value, expressing the number of methyl groups incorporated into DNA (0.5 μg DNA), represents the mean±SEM for six experiments with three simultaneous samples each.

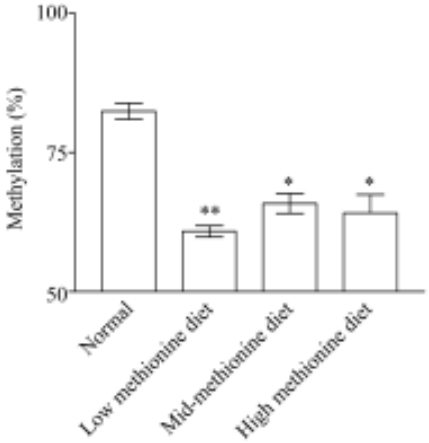


**Fig. 9 Levels of methylated B1 repetitive elements analyzed by real-time polymerase chain reaction**

**P*<0.05, ***P*<0.001 versus control.

converted DNA as a substrate. Each MethyLight-based methylation data point is expressed as the percent of methylated reference value using a CpG-independent, bisulfite-specific control reaction to measure input DNA levels. We found that the increase of the methionine diet concentration from 1% to 1.5%, and further to 2%, led to significant 26.2%, 20.1% and 22.2% ($P<0.05$) decrease, respectively, in genome hypomethylation in B1 repetitive elements (**Fig. 9**).

## Discussion

HHcy is a common and independent risk factor for atherosclerosis. Oxidative stress, apoptosis and inflammation are some of the mechanisms that have been implicated in Hcy-induced atherosclerosis, for which plenty of experimental evidence has been produced, but none has been definitively proven. Although the concentration of cysteine is approximately 20–25 folds higher than Hcy in patients with atherosclerosis, it is not usually considered a risk factor for cardiovascular diseases [25–

27]. Why did the Hcy become a pro-oxidant and an important risk factor for atherosclerosis? Many plausible explanations have not probed this key point.

In the methionine cycle, the methyl-group for DNA modification is provided by AdoMet, and catalyzed by DNA methyltransferase. After the methyl-group is transferred to DNA or other target compounds, the produced AdoHcy is then hydrolyzed to Hcy. Hcy can be recycled to methionine, or be eliminated by other metabolic pathways. So an abnormal increased Hcy concentration might interfere with this cycle, and result in impacts on AdoHcy hydrolase, AdoHcy, DNMT, AdoMet and the methylation status of gDNA. The present study aimed to address the potential epigenetic effects on methylation modulation of gDNA by HHcy and the intermediate factors involved in this process, which might help in gaining a better understanding of the molecular basis of Hcy-induced atherogenesis and understanding the different functions of Hcy and cysteine in atherogenesis.

Our results showed that an increased Hcy concentration induced elevation in AdoHcy, decline in AdoMet and the ratio of AdoMet/AdoHcy, reduction in the expression of AdoHcy and MBD2, increase in the activity of DNMT3a and 3b and the methylation status of gDNA, and down-grading of the DNA methylation level.

AdoHcy is favored in an equilibrium with adenosine and Hcy catalyzed by AdoHcy hydrolase and inhibits the activities of most S-adenosylmethionine-dependent methyltransferases [28–30]. Recently, a case of AdoHcy hydrolase deficiency was reported in which the patient's leukocyte DNA was hypermethylated relative to controls despite extreme levels of plasma AdoHcy [31]. Likewise, DNA from rat colon with high AdoHcy concentration has recently been noted to have methylation levels compared with those controls in three separate studies [32–34]. Our results showing that the activity of DNMTs increased and the expression level of MBD2 decreased were unexpected, because AdoHcy is an inhibitor of many AdoMet-dependent methyltransferases such as DNMTs. A potential yet plausible explanation was the compensatory reaction of the methylation machinery against Hcy-induced hypomethylation. It has been reported that methyl-transferase activity in cancer tissue was actually increased in spite of the genome-wide hypomethylation [35]. Methyltransferase activity can be seen as a compensatory mechanism to maintain genomic methylation patterns, as only two rounds of replications are required for genomic hypomethylation if maintenance methylation activity provided by DNMT or other methyltransferases is not operative. The decline of AdoMet could result from excessive consumption due to increased activity of DNMT [36].

gDNA hypomethylation might serve as a mechanistic link between HHcy and atherosclerosis. Further work is needed to characterize gene-specific hypermethylation and hypomethylation as opposed to DNA hypomethylation in the presence of HHcy and the significance of such hypermethylation in consequent atherosclerosis [37–39]. Methylation-dependent restriction endonucleases, which recognize unmethylated cytosine, can cut certain specific CG sequences but not the methylated mCG. *Hpa*II, specific for CCGG sequences and *Bss*HII, specific for CpG islands (CGCGCG) were used in this experiment for investigating the Hcy-induced alteration in DNA methylation and its potential sequence bias. Digestion with *Hpa*II or *Bss*HII restriction endonucleases resulted in a destruction of corresponding CpG loci and loss of the potential methylation-accepting sites. A smaller decline of methyl-accepting capacity in *Bss*HII than *Hpa*II indicated a relatively lower level of demethylation in the sequence of *Bss*HII cutting loci, which recognized the CpG islands (CGCGCG). In the *Hpa*II group, the loss of methyl-accepting capacity was much greater than in *Bss*HII, because a higher demethylation induced by Hcy *Hpa*II recognizing loci would leave more unmethylated cytosines for *Hpa*II cutting, and methyl-accepting capacity was lost during *Hpa*II restriction analysis. The results strongly suggested that HHcy could lead to hypomethylation of gDNA, and this demethylation was preferentially biased for the CCGG sequence, not the CpG islands [40]. Although the CpG islands were found to be more closely associated with promoters of many genes, the aberrant methylation patterns in non-CpG island sequences induced by Hcy might also deeply influence the expression of genes, including the atherosclerosis-related genes, because maintenance of differential chromatin structure between transcriptionally competent, insulator and repressed genes were all critical aspects for transcriptional regulation.

The impacts of low, mid and high methionine diet groups on the one-carbon methyl-group transferring metabolism, however, did not show a dose-effect relationship. AdoMet and AdoHcy are the substrates and products of essential methyltransferase reactions, so the ratio of AdoMet/AdoHcy rather than AdoHcy is frequently used as an indicator of cellular methylation potential. The highest effects on aberrant methylation of DNA, factors involved in the pathway of DNA methylation and AdoMet recycling were in the low methionine diet group. The increase of HHcy exerted weaker effects on the aberrant methylation of DNA and involved factors, which was unexpected,

but might be reasonable. The high methionine diet group might exert more direct injurious effects such as oxidative stress and apoptosis, whereas the moderate HHcy might show milder impacts on the epigenetic modulation of gene expression [41-43]. This phenomenon suggested that the varied detrimental effects of Hcy could be attributed to different concentrations using different mechanisms, for example, in mild and moderate HHcy, Hcy might primarily influence the epigenetic regulation of gene expression through the interference of methyl-group transferring metabolism. However, in much higher Hcy concentrations, the essential impacts might be more directly injurious through oxidative stress, pro-apoptosis or inflammation.

Our findings uncovered Hcy-induced DNA hypomethylation. The increased activity of DNMT was similar to that seen in cancer tissues. It is possible that alterations in DNA methylation might play important roles in atherogenesis, showing a direct relationship between hypomethylation and atherogenesis. Our results also indicated a sequence bias in Hcy-induced hypomethylation for CCGG, but not for CpG islands. Results suggested that different concentrations of Hcy might exert different effects using different mechanisms. So the interventions directed towards Hcy in the treatment for vascular disorders should be more specific according to the different concentrations and mechanisms. This fact might be significant for therapy of atherogenesis that is associated with gene silencing due to hypermethylation of their regulatory regions. The induction of DNA methylation by HHcy is a new, hitherto unreported element of their mechanisms and these findings reveal a novel role of Hcy in the pathogenesis of human vascular disease.

## References


1 Selhub J, Miller JW. The pathogenesis of homocysteinemia: Interruption of the coordinate regulation by S-adenosylmethionine of the remethylation and transsulfuration of homocysteine. Am J Clin Nutr 1992, 55: 131–138

2 Clarke R, Daly L, Robinson K. Hyperhomocysteinemia: An independent risk factor for vascular disease. N Engl J Med 1999, 324: 1149–1155

3 Riba R, Nicolaou A, Troxler M. Altered platelet reactivity in peripheral vascular disease complicated with elevated plasma homocysteine levels. Atherosclerosis 2004, 175: 69–75

4 Refsum H, Ueland PM, Nygard O. Homocysteine and cardiovascular disease. Annu Rev Med 1998, 49: 31–62

5 Feinberg AP, Tycko B. The history of cancer epigenetics. Nat Rev Cancer 2004, 4: 143–153

6 Yi P, Melnyk S, Pogribna M, Pogribny IP, Hine RJ, James SJ. Increase in plasma homocysteine associated with parallel increases in plasma S-adenosylhomocysteine and lymphocyte DNA hypomethylation. J Bio Chem 2000, 275: 29318–29323

7 Friso S, Choi SW, Girelli D, Mason JB, Dolnikowski GG, Bagley PJ, Olivieri O *et al*. A common mutation in the 5,10-methylenetetrahydrofolate reductase gene affects genomic DNA methylation through an interaction with folate status. Proc Natl Acad Sci USA 2002, 99: 5606–5611

8 Ingrosso D, Cimmino A, Perna AF, Masella L, De Santo NG, De Bonis ML, Vacca M *et al*. Folate treatment and unbalanced methylation and changes of allelic expression induced by hyperhomocysteinaemia in patients with uraemia. Lancet 2003, 361: 1693–1699

9 Hiltunen MO, Turunen MP, Hakkinen TP, Rutanen J, Hedman M, Mäkinen K, Turunen AM *et al*. DNA hypomethylation and methyltransferase expression in atherosclerotic lesions. Vasc Med 2002, 7: 5–11

10 Hiltunen MO, Yla-Herttuala S. DNA methylation, smooth muscle cells, and atherogenesis. Arterioscler Thromb Vasc Biol 2003, 23: 1750–1753

11 Devlin AM, Bottiglieri T, Domann FE, Lentz SR. Tissue-specific changes in H19 methylation and expression in mice with hyperhomocysteinemia. J Biol Chem 2005, 280: 2550625511

12 Patra SK, Patra A, Zhao H. DNA methyltransferase and demethylase in human prostate cancer. Mol Carcinog 2002, 33: 163–171

13 Pogribny I, Yi P, James SJ. A sensitive new method for rapid detection of abnormal methylation patterns in global DNA and within CpG islands. Biochem Biophys Res Commun 1999, 262: 624–628

14 Weiner AM. SINEs and LINEs: The art of biting the hand that feeds you. Curr Opin Cell Biol 2002, 14: 343–350

15 Deininger PL, Moran JV, Batzer MA. Mobile elements and mammalian genome evolution. Curr Opin Genet Dev 2003, 13: 651–658

16 Prak ET, Kazazian HH Jr. Mobile elements and the human genome. Nature Rev Genet 2000, 1: 134–144

17 Yates PA, Burman RW, Mummaneni P, Krussel S, Turker MS. Tandem B1 elements located in a mouse methylation center provide a target for *de novo* DNA methylation. J Biol Chem 1999, 274: 36357–36361

18 Jeong KS, Lee S. Estimating the total mouse DNA methylation according to the B1 repetitive elements. Biochem Biophys Res Commun 2005, 335: 1211–1216

19 Jones PA, Laird PW. Cancer epigenetics comes of age. Nat Genet 1999, 21: 163–167

20 Dong C, Yoon W, Goldschmidt-Clermont PJ. DNA methylation and atherosclerosis. J Nutr 2002, 132: S2406–S2409

21 Post WS, Goldschmidt-Clermont PJ, Wilhide CC. Methylation of the estrogen receptor gene is associated with aging and atherosclerosis in the cardiovascular system. Cardiovasc Res 1999, 43: 985–991

22 Quere I, Hillaire-Buys D, Brunschwig C. Effects of homocysteine on acetylcholine- and adenosine-induced vasodilatation of pancreatic vascular bed in rats. Br J Pharmacol 1997, 122: 351–357

23 Mudd SH, Finkelstein JD, Refsum H. Homocysteine and its disulfide derivatives: A suggested consensus terminology. Arterioscler Thromb Vasc Biol 2000, 20: 1704–1706

24 Bottiglieri T. Isocratic high performance liquid chromatographic analysis of *S*-adenosylmethionine and *S*-adenosylhomocysteine in animal tissues: The effect of exposure to nitrous oxide. Biomed Chromatogr 1990, 4: 239–241

25 Bensadoun A, Weinstein D. Assay of proteins in the presence of interfering materials. Anal Biochem 1976, 70: 241–250

26 Wyczechowska D, Fabianowska-Majewska K. The effects of cladribine and fludarabine on DNA methylation in K562 cells. Biochem Pharmacol 2003, 65: 219–225

27 Zeschnigk M, Böhringer S, Price EA, Onadim Z, Masshöfer L, Lohmann DR. A novel real-time PCR assay for quantitative analysis of methylated alleles (QAMA): Analysis of the retinoblastoma locus. Nucleic Acids Res 2004, 32: e125

28 Lavigne MC, Ramwell PW, Clarke R. Growth and phenotypic characterization of porcine coronary artery smooth muscle cells. In Vitro Cell Dev Biol

Anim 1999, 35:136–143
29 Durga J, Verhoef P, Bots ML. Homocysteine and carotid intima-media thickness: A critical appraisal of the evidence. Atherosclerosis 2004, 17: 1–19
30 Hoffman DR, Marion DW, Cornatzer WE, Duerre JA. *S*-adenosylmethionine and *S*-adenosylhomocystein metabolism in isolated rat liver. Effects of *L*-methionine, *L*-homocystein, and adenosine. J Biol Chem 1998, 255: 10822–10827
31 Baric I, Fumic K, Glenn B, Cuk M, Schulze A, Finkelstein JD, James SJ *et al.* S-adenosylhomocysteine hydrolase deficiency in a human: A genetic disorder of methionine metabolism. Proc Natl Acad Sci USA 2004, 101: 4234–4239
32 Davis CD, Uthus EO. Dietary folate and selenium affect dimethylhydrazine-induced aberrant crypt formation, global DNA methylation and one-carbon metabolism in rats. J Nutr 2003, 133: 2907–2914
33 Sohn KJ, Stempak JM, Reid S. The effect of dietary folate on genomic and p53-specific DNA methylation in rat colon. Carcinogenesis 2003, 24: 81–90
34 Choi SW, Friso S, Dolnikowski GG, Bagley PJ, Edmondson AN, Smith DE, Mason JB. Biochemical and molecular aberrations in the rat colon due to folate depletion are age-specific. J Nutr 2003, 133: 1206 –1212
35 Haaf T. The effects of 5-azacytidine and 5-azadeoxycytidine on chromosome structure and function: Implications for methylation-associated cellular processes. Pharmacol Ther 1995, 65: 19–46
36 Lee PJ, Washer LL, Law DJ. Limited up-regulation of DNA methyltransferase in human colon cancer reflecting increased cell proliferation. Proc Natl Acad Sci USA 1996, 93: 10366–10370
37 Wilson AS, Power BE, Molloy PL. DNA hypomethylation and human diseases. Biochim Biophys Acta 2007, 1775: 138–162
38 Poirier LA. The effects of diet, genetics and chemicals on toxicity and aberrant DNA methylation: An introduction. J Nutr 2002, 132: S2336–S2339
39 Ying AK, Hassanain HH, Roos CM, Issa JJ, Michler RE, Caligiuri M, Plass C *et al.* Methylation of the estrogen receptor-α gene promoter is selectively increased in proliferating human aortic smooth muscle cells. Cardiovasc Res 2000, 46: 172–179
40 White GP, Watt PM, Holt BJ. Differential patterns of methylation of the IFN-γ promoter at CpG and non-CpG sites underlie differences in IFN-γ gene expression between human neonatal and adult CD45RO-T cells. J Immunol 2002, 168: 2820–2827
41 Hatzistamou J, Kiaris H, Ergazaki M. Loss of heterozygosity and microsatellite instability in human atherosclerotic plaques. Biochem Biophys Res Commun 1996, 225: 186–190
42 Jiang Y, Zhang Jian, Juan Y, Zhang J, Wang L, Han X, Wang S. Homocysteine-mediated aberrant DNA methylation in vascular smooth muscle cells and its potential pathogenic mechanism. Prog Biochem Biophys 2007, 34: 479–489
43 Jiang Y, Zhang J, Xiong J, Cao J, Li G, Wang S. Ligands of peroxisome proliferator-activated receptor inhibit homocysteine-induced DNA methylation of inducible nitric oxide synthase gene. Acta Biochim Biophys Sin 2007, 39: 366–376

Edited by
**Guoliang XU**